The Journal of Experimental Biology 210, 2730-2742
Published by The Company of Biologists 2007
doi:10.1242/jeb.001784

The functional architecture of the shark's dorsal-octavolateral nucleus: an *in vitro* study

Naama Rotem[1], Emanuel Sestieri[1], Dana Cohen[2], Mike Paulin[3], Hanoch Meiri[4] and Yosef Yarom[1,4,*]

[1]The Otto Loewi Center, the Inter University Institute, Eilat, Israel, [2]The Gonda Interdisciplinary Brain Research Center, Bar Ilan University, Ramat Gan, Israel, [3]Department of Zoology and Centre for Neuroscience, University of Otago, Dunedin, New Zealand and [4]Department of Neurobiology, the Institute of Life Sciences, Hebrew University, Jerusalem, 91904, Israel

*Author for correspondence (e-mail: Yarom@vms.huji.ac.il)

Accepted 16 May 2007

Summary

Learning to predict the component in the sensory information resulting from the organism's own activity enables it to respond appropriately to unexpected stimuli. For example, the elasmobranch dorsal octavolateral nucleus (DON) can apparently extract the unexpected component (i.e. generated by nearby organisms) from the incoming electrosensory signals. Here we introduce a novel and unique experimental approach that combines the advantages of *in vitro* preparations with the integrity of *in vivo* conditions. In such an experimental system one can study, under control conditions, the cellular and network mechanisms that underlie cancellation of expected sensory inputs.

Using extracellular and intracellular recordings we compared the dynamics and spatiotemporal organization of the electrosensory afferent nerve and parallel fiber inputs to the DON. The afferent nerve has a low threshold and high conduction velocity; a stimulus that recruits a small number of fibers is sufficient to activate the principal neurons. The excitatory postsynaptic potential in the principal cells evoked by afferent nerve fibers has fast kinetics that efficiently reach the threshold for action potential. In contrast, the parallel fibers have low conduction velocity, high threshold and extensive convergence on the principal neurons of the DON. The excitatory postsynaptic response has slow kinetics that provides a wide time window for integration of inputs.

The highly efficient connection between the afferent nerve and the principal neurons in the DON indicates that filtration occurring in the DON cannot be mediated simply by summation of the parallel fibers' signals with the afferent sensory signals. Hence we propose that the filtering may be mediated *via* secondary neurons that adjust the principal neurons' sensitivity to afferent inputs.

Key words: dorsal-octavolateral, nucleus, electrophysiology, electroreception, shark, synaptic interactions.

Introduction

The ability of a living organism to respond appropriately to external stimuli depends on its ability to discern sensory inputs arriving from external sources from those generated by its own movement. In fact, it is part of a fundamental characteristic of an organism to distinguish self from non-self. The neuronal circuitry in the mammalian brain that underlies this ability remains to a large extent unknown (Devor, 2000). However, the suggestion that cerebellar-like hindbrain circuitry performs this function in the electrosensory system of elasmobranches has been supported by experimental evidence for more than two decades (Bodznick et al., 2003; Montgomery, 1984; Montgomery and Bodznick, 1994).

In the electrosensory system of elasmobranches the dorsal-octavolateral nucleus (DON) is the site where unexpected sensory input is retrieved from the overall sensory information. The DON is a structure in the medulla that serves as the first stage that processes sensory information. It receives direct inputs from the peripheral electroreceptors – the ampullae of Lorenzini – *via* the afferent nerve (Aff) known as the superficial opthalmic ramus of the anterior lateral line nerve. The information conveyed by the afferent nerve comprises the electrical field generated by the elasmobranch's own movements (reafferent signals) and electrical fields generated by external sources. In the output of the DON, transmitted by the axon of the ascending efferent neurons (AENs), the reafferent signals are significantly attenuated, and information about electrical fields generated by the external sources is enhanced. Hence, it has been hypothesized that the DON predicts self-generated electrosensory information and subtracts it from the incoming sensory information, thus leaving essential sensory information about possible prey intact (Montgomery and Bodznick, 1999; Bodznick et al., 2003).

The DON is a cone-shaped structure divided into three layers organized along the dorso-ventral axis. The principal cell layer, located at the center of the DON, is composed of the AENs. The AENs have extensive dendritic arborizations, spreading ventrally and dorsally to form the ventral and dorsal dendrites,

respectively. The ventral dendrites of the AEN receive monosynaptic input from the terminals of the Aff, thus forming the afferent fiber layer. The dorsal dendrites spread dorsally into the molecular layer where they are innervated by the parallel fibers (PF) (Paul and Roberts, 1977). Inhibitory interneurons have been described in both the Aff layer and the molecular layer (Montgomery and Bodznick, 1994; Paul et al., 1977). The PF of the DON, which arise from a mass of granular cells forming the dorsal granular ridge (DGR), carry three categories of information: proprioceptive information, reflecting body movements; descending electrosensory information and corollary discharge signals associated with the motor commands (Bell, 2002).

The term 'adaptive filter' has been used to denote the ability of the DON to filter out the irrelevant, namely the expected, sensory information. It has been suggested that plasticity in the PF synapses underlies the adaptive capabilities of the filtration process. Specifically, when PF input precedes or coincides with AEN action potential, the strength of the PF synapse is supposedly decreased, allowing adaptive filtration of the electrosensory information. This adaptive filtering, which is anti-Hebbian in nature, decreases AEN output in correlation with the activity in the PF.

Knowledge about functional signal processing in the DON has been derived from *in vivo* preparations. In order to gain insight into the cellular and network mechanisms underlying the adaptive filtering properties of the DON, we developed a unique *in vitro* preparation of a shark (*Iago omanensis*) brainstem, consisting of the DON and the afferent nerve originating at the Ampullae of Lorenzini. This preparation allows us to examine anatomical and electrophysiological properties of the intact DON and its afferents. Specifically, we characterize the temporal and spatial propagation of local field potential (LFP) reflecting inhibitory and excitatory responses to stimulation of the Aff and the PF.

Materials and methods

Animals

60 Adult *Iago omanensis* Norman 1939 sharks were caught in the Gulf of Eilat, from a depth range of 400–800 m. Sharks, 30–60 cm in length, were collected at night, using a red light source to prevent eye damage, and kept at 20°C in a dark seawater pool with fresh seawater circulation rate of 20% in 24 h.

Surgical procedure

Sharks were immobilized by cooling to 8–10°C. Following decapitation, at the level of the first gill, the cartilaginous skull containing the brain was removed and immersed in a 7–10°C shark Ringer solution. As shown in Fig. 1A, the cartilaginous bone was carefully removed to expose the cerebellum (green), the brain stem (white), the spinal cord (yellow) and the cranial nerves. Subsequently the brainstem and the Aff were isolated from the level of the dorsal granular ridge (DGR, Fig. 1B,C) to the level of cervical vertebrate (c3). The isolated brainstem was incubated in the experimental chamber, which was continuously superfused with aerated cold (15°C) Ringer solution for at least 1 h prior to recording. During incubation, the temperature was gradually increased to 20°C, the temperature of the *Iago omanensis* natural habitat.

Shark Ringer solution (modified from Hentschel et al., 2003), contained (in mmol l^{-1}) 280 NaCl, 6 KCl, 5 $CaCl_2$-$2H_2O$, 3 $MgCL_2$-$6H_2O$, 0.5 Na_2SO_4, 1 NaH_2PO_4-$12H_2O$, 8 $NaHCO_3$, 350 urea,

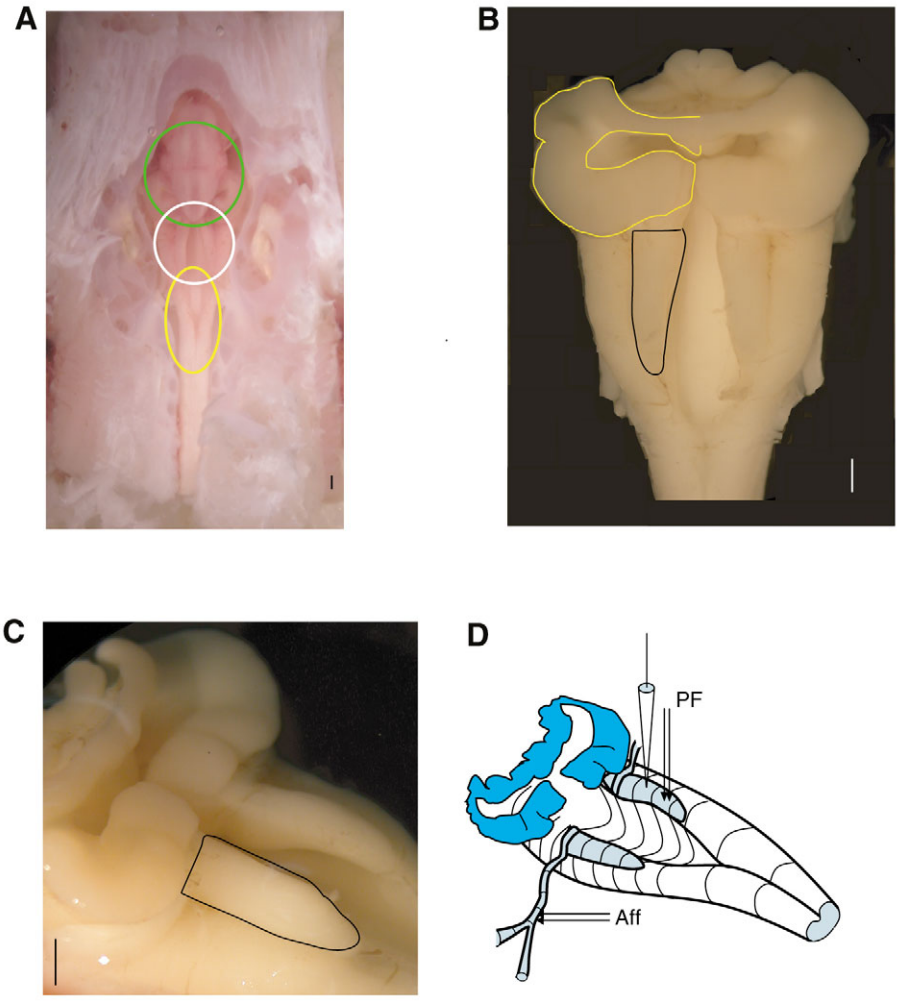

Fig. 1. The isolated brain stem of the shark *Iago omanensis*. (A) Careful removal of the cartilage skull completely exposed the brain stem (white circle), the cerebellum (green circle) and the cervical spinal cord (yellow circle). (B) Top view of the shark's isolated brain stem. The black and yellow lines outline the DON and the dorsal granular ridge (DGR), respectively. (C) Side view of the shark's isolated brain stem where the DON is marked by black line. (D) Schematic drawing of the isolated preparation, showing the relative locations of the stimulating and the recording electrodes. PF, parallel fibers; Aff, afferent nerve. Scale bars in A–C, 1 mm.

72 trimethylamine *N*-oxide dehydrate (TMAO, Sigma, Rehovot, Israel), 5 glucose, 0.75 polyvinylpyrrolidone (PVP-40T, Sigma). The pH of this modified Ringer solution was 7.4–7.6.

The isolated preparation is shown in Fig. 1B,C. Continuous lines outline the DON (black) and the DGR (yellow). A schematic illustration of the isolated preparation (Fig. 1D) was reconstructed from images such as those shown in Fig. 1B,C. The locations of the stimulating and the recording electrodes were marked. To the best of our knowledge this is the first isolated intact preparation of the DON. This unique preparation maintains the integrity of the network, which is extremely advantageous over the commonly used *in-vitro* slices when studying network connectivity and integration in the DON.

Electrophysiological recording

4–7 MΩ electrodes filled with 2 mol l^{-1} NaCl were used to measure local field potentials (LFP) *via* an amplifier (Axoclamp 2A, Foster City, CA, USA). Homemade bipolar electrodes were prepared from Teflon coated, 75 μm diameter silver wires. The wires were wrapped together so that the two exposed tips were separated by 100 μm. These stimulating electrodes were placed either on the ipsilateral afferent nerve or on the dorsal surface of the DON. Since the entire preparation is continuously immersed in the physiological solution the tips of both electrodes were also immersed. The stimulating electrodes were driven by 0.1 ms pulses, of various intensities. In experiments where bicuculline was used to block $GABA_A$ receptors, it was added to the external solution reaching a final concentration of 50–100 μmol l^{-1}, and recording started 30 min after initial bicuculline application. Sharp glass pipettes filled with 2 mol l^{-1} potassium acetate (30–60 MΩ) were used for intracellular recordings. For intracellular labeling, the electrodes were filled with 5% neurobiotin (Sigma) diluted in 1 mol l^{-1} potassium acetate. These electrodes had a d.c. resistance of 60–80 MΩ. Positive current pulses of 0.5–1.2 nA in amplitude, 50 ms duration repeated at 1 Hz for 10–60 min were used to deliver the neurobiotin into the cells.

Histological procedures

Following neurobiotin injection, the isolated brain stem was fixed for 24 h, imbedded in a gelatin block (made of 7% gelatin solution) and incubated for 48 h in the fixative solution. The fixative solution consisted of 4% formaldehyde diluted in 730 mmol l^{-1} phosphate buffer solution (PBS). 200 μm cross-section slices were cut by a vibratome and immersed in PBS for 30 min. The free-floating sections were 'prebleached' by soaking for 20 min in 0.5% H_2O_2 in PBS. The sections were then washed 3× and incubated in ABC solution for 4–6 h [2 drops A+2 drops B in 5 ml PBS (ABC Standard Elite Kit, Vector Labs, Burlingame, CA, USA)]. After thorough washing in PBS, the sections were incubated for 10–15 min in a solution containing 5 mg diaminobenzidine (DAB; Sigma), 20 ml PBS, 1 ml 0.3% NiCl and 5 μl H_2O_2. The reaction was stopped by washing in PBS. Sections were mounted onto chrome alum gelatin-coated slides and left to dry overnight. Slides were then immersed in a series of alcohol and xylene for dehydration and clearness.

Data analysis

Data acquisition board (PCI-MIO-16XE-10, National Instruments, Austin, TX, USA), controlled by software written in LabView (National Instruments), was used to sample the data at a rate of 10 000 samples s^{-1} and stored for offline analysis. The LFP recorded traces were averaged 5–10 times before storing and the subthreshold synaptic potentials were occasionally averaged five times. The amplitude of the LFP response was measured from the positive peak to its following negative peak. The durations of the negative and positive components were measured between the points at which the potential reversed its polarity. The delay was measured from stimulus onset to the negative peak in the response. The amplitudes of both the action potentials and the synaptic potentials were measured from the resting potential to the peak of the response and their duration was measured at half amplitude. The rise time of the synaptic potentials was measured from 10% to 90% of the amplitude.

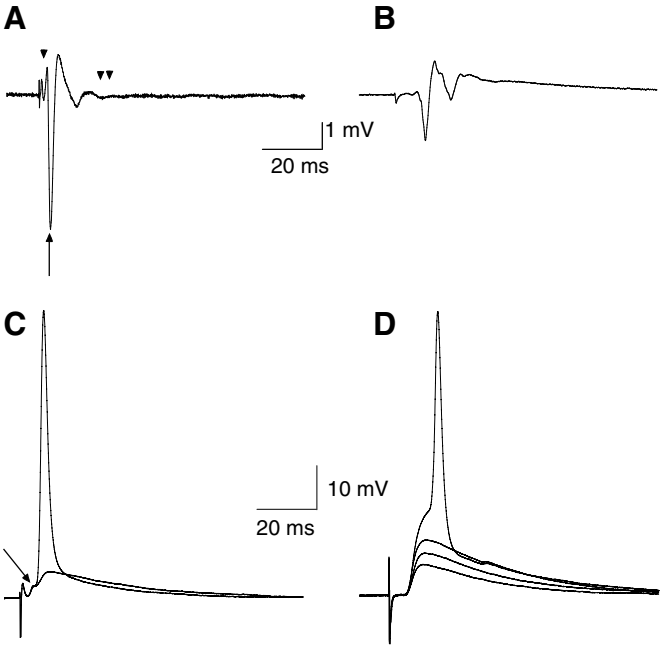

Fig. 2. Characterizing the responses elicited by stimulation of either the parallel fibers (PF) or the afferent nerve (Aff). (A,B) Extracellular recording of the responses to Aff (A) and PF (B) stimulation. Each record represents the average response to eight consecutive stimuli delivered at a rate of 0.1 Hz and recorded at a depth of 500 μm below the surface of the DON. (A) The response of the DON to Aff nerve stimulation is characterized by an early positive component (arrowhead); the main triphasic component is marked by an upward arrow and the second small negative component is marked by a double arrowhead. (B) The response of the DON to PF stimulation is characterized by significant longer delay, the pronounced second negativity and the overall longer duration of the PF response in compare to Aff response. (C,D) Intracellular recording of the responses to Aff (C) and PF (D) stimulation. (C) Sub- and supra-threshold responses to Aff stimulation recorded intracellularly. The subthreshold synaptic potential was occasionally composed of two depolarizing phases separated by a short delay (arrow). (D) Sub- and supra-threshold responses to PF stimulation recorded intracellularly. Note the higher threshold of the PF evoked action potential.

Results

Characterizing the responses elicited by stimulation of either the parallel fibers or the afferent nerve

The responses to stimulation of the afferent nerve (Aff) and of the parallel fibers (PF) were characterized at the population level by measuring the LFP and at the single cell level by intracellular recordings. LFPs were measured in the middle portion of the DON at a depth of 500 μm, whereas individual neurons were impaled at various depths ranging between 100 and 600 μm below the molecular layer surface. An example of population responses to Aff and PF stimulations is shown in Fig. 2A,B and their corresponding intracellular activity is demonstrated in Fig. 2C,D.

Response shapes

The field potential evoked in response to the Aff stimulation (Fig. 2A) is characterized by a fast positive wave (arrowhead), which most likely reflects the propagation of the action potential volley in terminals of the Aff. This positive wave is followed by a triphasic slower response that reaches maximum negativity after 4.2 ms; an average delay of 4.36±0.81 ms (mean ± s.d.) was measured in 13 preparations. The triphasic response probably reflects somatic action potentials (maximum negativity marked with an arrow) superimposed on the synaptic currents (positive slow wave). Occasionally, the characteristic triphasic response was followed by another small negative component (double arrowhead) (see also Fig. 9D), suggesting that a single peripheral stimulation can elicit a short burst of postsynaptic action potentials. On average, the amplitude of the triphasic response was 2.76±1.44 mV (*N*=15). The average duration of the negative and the second positive components were 2.91±0.7 ms and 5.45±1.07 ms, respectively (*N*=13).

A considerably different response was observed when the PF were stimulated (Fig. 2B). At a depth of 500 μm the response appeared after an average delay of 8.8±2.6 ms (*N*=18) and was characterized by a fast negativity followed by a prolonged positive wave on which a second, and sometimes several, sharp negative wavelets were observed. On average the amplitude of the response was 1.4±0.8 mV. The average durations of the negative and positive components were 3.8±0.7 ms and 62±20 ms, respectively.

The longer delay of the response to PF stimulation and the shorter distance to the stimulating electrode compared to Aff stimulation suggests that the PF have slower conduction velocities. The conduction velocity was estimated by measuring the difference in the delay of the response after relocating the stimulating electrode along the activated axons. The average conduction velocities of the PF and the Aff were 0.13±0.04 m s^{-1} and 10.3±4.4 m s^{-1}, respectively. In addition, the response duration to PF stimulation was an order of magnitude longer than that of the Aff stimulation, suggesting that PF synapses have a slower kinetics than that of Aff synapses.

In contrast to the differences in response delays and response durations, the negative wave in the two responses had a similar shape, suggesting that both stimuli activated the same population of postsynaptic elements. The different amplitude of the two negative waves suggests that the two inputs either activate the DON to a different extent or to a different level of synchronization.

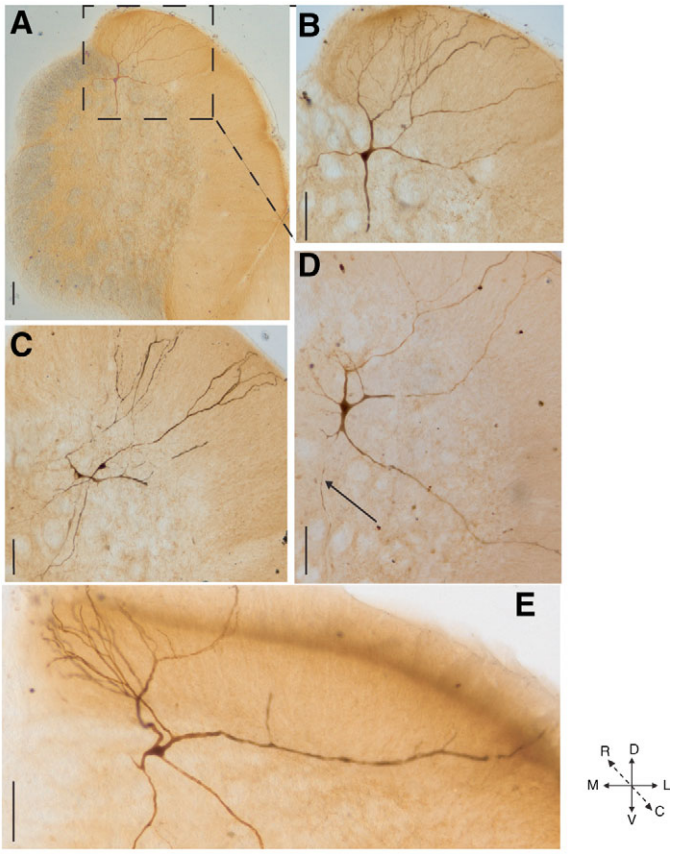

Fig. 3. Intracellular labeling of the ascending efferent neurons (AEN) of the DON. (A–E) Unstained cross sections through the middle portion of the DON developed for neurobiotin staining. (A) A low-power micrograph capturing the entire DON. The molecular layer appeared as a homogenous tissue lightly stained in brownish color. The principal cell layer appeared as a granular tissue with occasionally spherical structures. This difference forms a clear-cut border between the two compartments of the DON. (B) An enlarged view of the area outlined in A, focusing on the labeled cell. (C–E) Several examples of labeled neurons. The presume axon in C is marked with an arrow. Note that the overall orientations of the cells are along the medio-lateral axis. All of them emit a rather extensive dendritic tree that bifurcates dorsally into the molecular layer and ventrally into the DONs principal cell layer. Scale bar, 100 μm. D, dorsal; V, ventral; L, lateral; M, medial; R, rostral; C, caudal.

Intracellular recordings were performed from 95 neurons, of which 62 cells responded to both inputs. From the population of neurons that respond to both inputs we selected 32 that showed a resting potential more negative than –50 mV and an action potential larger than 50 mV for further analysis. The average resting potential and average action potential were –69.2 mV and 63 mV (*N*=32), respectively. In all the neurons the synaptic potentials evoked by both inputs gradually increased with stimulus intensity until threshold is reached and action potentials are generated. (Fig. 2C,D). This finding confirms the conclusion that there is a population of neurons within the DON activated by both inputs. Aff stimulation (Fig. 2C) was characterized by a rather low amplitude synaptic potential, occasionally composed of two depolarizing phases separated by a short delay. Threshold was reached at a rather

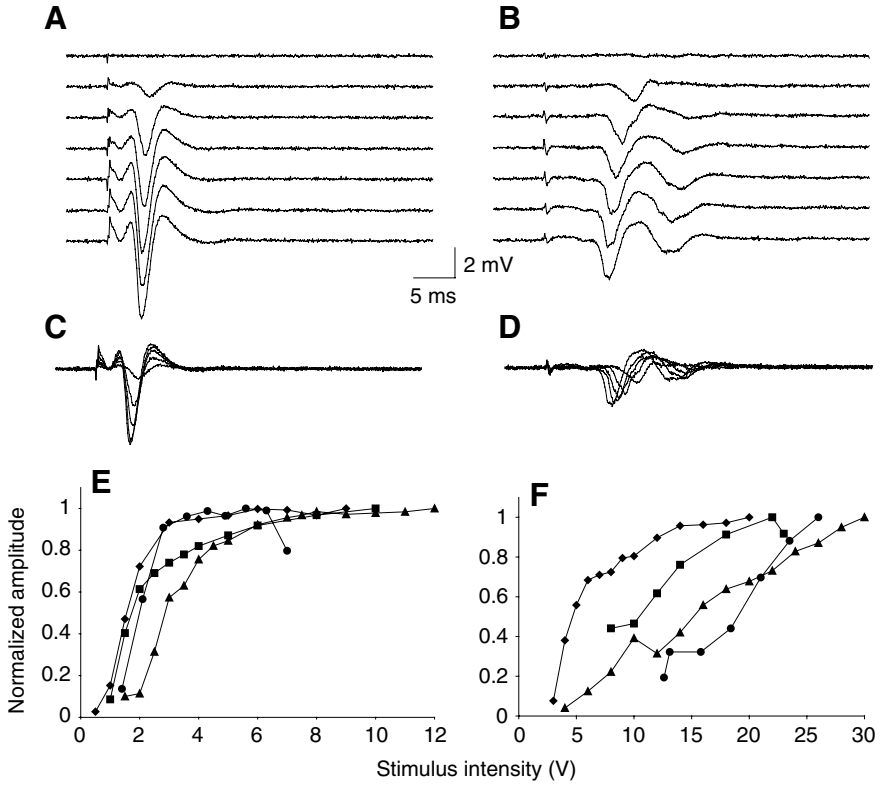

Fig. 4. The afferent nerve (Aff) has a lower threshold and a shorter dynamic range of stimulation than the parallel fibers (PF). (A,B) The responses to Aff and PF stimulation, respectively, following increase in stimulus intensity (from top to bottom). Each record is an average response to eight consecutive stimuli delivered at a rate of 0.1 Hz and recorded at a depth of 500 μm below the surface of the DON. (C,D) Superposition of the responses shown in A and B, respectively. Note the change in delay of the response to PF stimulation. (E,F) Amplitude of the responses to Aff stimulation and PF stimulation, respectively, as a function of the stimulus intensity. The amplitude of the response in each experiment was normalized by the maximal amplitude (*N*=4; each symbol represents one experiment). Note the different scale of the *x*-axes; hence, the threshold of the PF is higher than that of the Aff nerve.

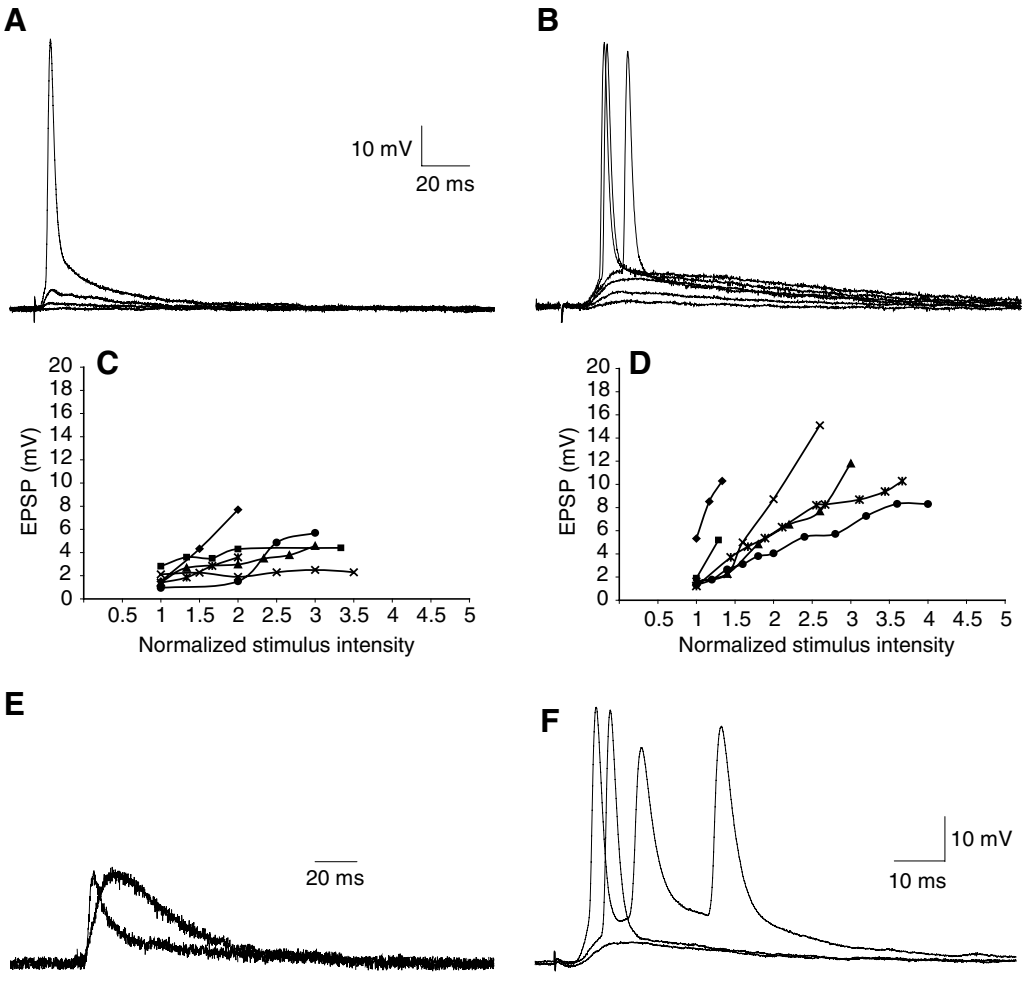

Fig. 5. Intracellular recordings showing the lower threshold and the shorter range of stimulations of the Aff. (A,B) The responses to Aff (A) and PF (B) stimulation following increased stimulus intensity. (C,D) Amplitude of the synaptic potential as a function of stimulus intensity for Aff (C) and PF (D) stimulation. The stimulus intensity in each experiment (*N*=6) was normalized by the threshold of detectable response. Each symbol corresponds to the behavior of one neuron for both inputs. Note that the range of Aff stimuli is considerably shorter than that of PF stimulation. (E) Superimposed normalized traces of the synaptic response to Aff and PF stimulation. Note the fast rise time of the Aff synapse compared to the PF synapse. (F) Increase in PF stimulus intensity evoked a prolonged response that can support the generation of a short burst of action potentials.

low intensity (see Fig. 5) and the response decayed within 70 ms, according to what seems to be the membrane time constant. The average half duration of the first phase of the Aff synaptic response was 17.4±7.8 ms and the duration of the combined phases was 31.5±6.4 ms. The differences recorded in the LFP responses of the two populations were manifested also in the intracellular recordings. The synaptic potential evoked by PF stimulation appeared after a longer delay, had a rather slow onset and the threshold to evoked postsynaptic action potential seemed to be higher (see Figs 5 and 6). The pronounced second negative wave in the field potential was always encountered at high stimulus intensities (Fig. 5F). The average duration of the PF evoked synaptic potential was 36±15.1 ms (N=20).

The identity of the postsynaptic neurons was established by intracellular labeling (see Materials and methods). Fig. 3 shows five neurons that were filled with neurobiotin. Indeed, these neurons share common features. First, as demonstrated in a lower power micrograph (Fig. 3A), they are located at the border between the molecular layer and the principal cell layer. Second, they are oriented at a similar plane as evident in Fig. 3C showing two labeled neurons. Third, all of them have a rather extensive dendritic tree that ramifies dorsally into the molecular layer and ventrally into the DON's principal cell layer. The dorsal dendritic tree is more elaborate in terms of number of primary dendrites and their secondary and tertiary bifurcations. Usually there are only two ventral dendrites that rarely bifurcate (Fig. 3B,D,E) compared with 3–5 dorsal dendrites that form a complex planar dendritic tree reminiscent of the Purkinje cell dendrite. Fourth, dendritic spines could not be identified. Fifth, presumed axons were occasionally identified as a fine homogeneous process that travels ventrolaterally without bifurcations into the output track of the DON (arrow in Fig. 3D). Since all the labeled neurons responded to both inputs we assume that most of our intracellular recordings were made from the AEN, the DON principal neurons.

The response amplitude

As expected, the amplitude of the PF and the Aff responses increased with stimulus intensity (Fig. 4A,B). A more careful analysis of these two responses revealed that they differed in four distinctive features. (1) The response to Aff stimulation was detected at lower stimulus intensities compared to PF stimulation (compare Fig. 4E and F; note the different scale). This can be attributed to the low threshold of the Aff, as expected in myelinated fibers. Alternatively, the low threshold of the response can be explained by a small number of Aff fibers needed to elicit a detectable response in the DON. (2) The delay following PF stimulation decreased as stimulus intensity increased (Fig. 4D), whereas the delay following Aff stimulation was less dependent on stimulus intensity (Fig. 4C). This difference is likely to reflect a slow rise time of the PF synaptic response. (3) The second negative wave in the response to PF input appeared at a lower stimulus intensity than that of the Aff input. This rather low activation threshold of the second response to PF input suggests a slow decay time of PF synapses. Based on the slow rise time and slow decay time of the PF synapse we suggest that this input has slow kinetics. (4) The response to Aff stimulation saturated within a short range of stimulus intensities, whereas the PF response rarely saturated and seemed to increase linearly within a wide range of stimulus intensities. This difference in saturation levels also supports the possibility that activation of a smaller number of Aff fibers is sufficient to activate the DON whereas more PF need to be activated in order to generate a detectable response in the DON.

These four features that distinguished the PF and the Aff inputs were further examined by analyzing the responses recorded intracellularly. The results are summarized in Fig. 5. The postsynaptic response to both PF and Aff activation increased in amplitude with stimulus intensity, eventually reaching the threshold and eliciting an action potential (Fig. 5A,B). Six experiments are summarized in the plots shown in Fig. 5C,D. The range of stimulus intensities of the Aff that evoked sub-threshold synaptic potentials was much smaller than that of PF stimulation. As a result there is a narrow distribution of the amplitude of the synaptic potential. This limited range of Aff sub-threshold activity, further supports the possibility that only a small number of Aff fibers converges on a single AEN neuron. Furthermore, these plots show that the depolarization required to evoke an action potential by Aff input is smaller than that of PF input (see Fig. 6). This difference can be due either to the existence of two distinct spike generating mechanisms or the site of action potential generation being closer to the Aff input and distal to the recording site. The intracellular recording also confirmed the lower threshold for the second response and

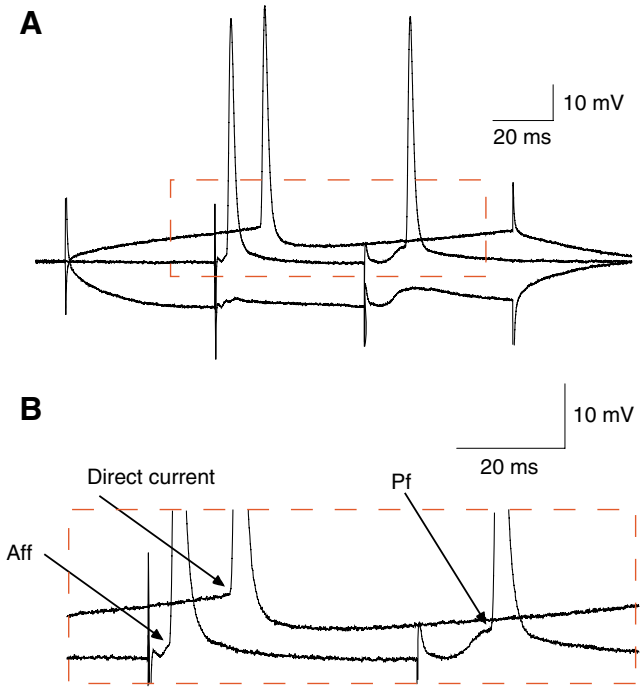

Fig. 6. The different thresholds for action potential generation. (A) Middle trace: intracellular recordings of the responses to just threshold, afferent nerve (Aff) and parallel fibers (PF) stimulation at resting membrane potential. Lower trace: the two responses were superimposed on voltage hyperpolarization evoked by 1 nA negative current injection. Upper trace: the response to supra-threshold positive injection of 1 nA current. (B) The area marked in A (broken line) is displayed at higher gain in B. Arrows point toward the different thresholds (note the sharp transient deflections on the onset and offset of the current pulse, reflecting bridge balancing artifacts).

led to the conclusion that the second negativity detected in the LFP does indeed represent prolonged input into the AEN which, with high intensity, can elicit a compound response at the single cell level. This prolonged response, shown in Fig. 5F, suggests that the PF input activates an intrinsic conductance that can support the generation of a burst of action potentials. Activation of such an intrinsic conductance was validated by blocking the delayed response and the prolonged depolarization by hyperpolarizing the cell's membrane (not shown). Finally the possibility that the Aff input has a faster kinetics than the PF was directly confirmed by comparing these two inputs (Fig. 5E). The two responses were normalized and superimposed to show, beyond doubt, that the Aff input has a faster rise time. Summarizing the results from ten neurons revealed that the average Aff rise time was 3.9±1.8 ms and that of the PF was two times slower, averaging at 8.8±3.5 ms.

The action potential threshold

The intracellular recordings strongly suggest that the threshold to elicit action potential by Aff input is much lower than the threshold to elicit action potential by the PF input. This observation, in addition to being interesting in its own merit, touches a fundamental issue; the interaction between these two inputs is the suggested mechanism for cancellation of self-generated responses. Therefore, we directly compared the threshold for spike initiation by activating a neuron with three different inputs. The procedure is shown in Fig. 6. We stimulated the Aff nerve at just threshold intensity; this was followed by just threshold stimulation of the PF input. The two responses were then superimposed on a hyperpolarizing pulse that prevented the cell from firing, thereby revealing the threshold synaptic potentials. Then we used the intracellular current injection to activate the cell directly and measured the voltage threshold for spike initiation. The area marked by the broken line is displayed at higher gain in Fig. 6B, where the arrows point the different thresholds. Indeed in this example the threshold for direct current injection was 10 mV, that of the PF was 4.5 mV and the Aff threshold was only 2 mV. Summarizing the results from 11 cells shows that the average spike threshold for Aff input is 2.9±1.74 mV where as that of PF input is 12±5.58 mV and the direct current is 14.7±5.65 mV. Whereas the threshold for Aff is significantly lower than that of the PF ($P \ll 0.005$) the PF threshold did not differ from the threshold for direct current injection. The significance of this observation is elaborated in the discussion.

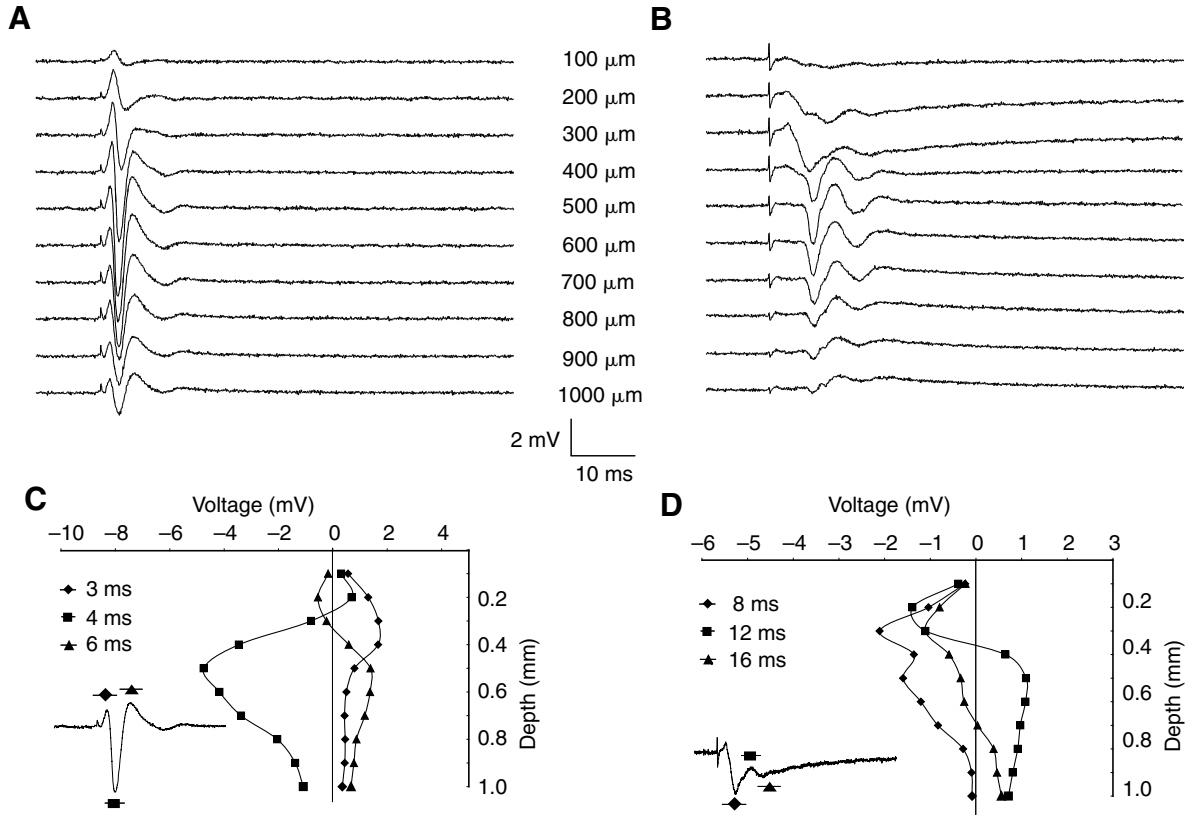

Fig. 7. The depth profile of the response to afferent nerve (Aff) and parallel fibers (PF) stimulation. (A,B) The responses to Aff nerve stimulation (A) and PF stimulation (B) at different locations along a single path of the microelectrode through the dorsal ventral axis of the DON. Each record is an average response to eight consecutive stimuli delivered at a rate of 0.1 Hz. The depth from the DON surface is indicated. (C,D) The changes in the responses to Aff (C) and PF (D) stimulation, as a function of the depth of recording. The relative voltage was measured at three times along the response as indicated on the corresponding insets. In C, the voltage was measured at 3, 6 and 8 ms from the time of stimulation and it is represented as diamonds, squares and triangles, respectively. In D, the voltage was measured at 8, 12 and 16 ms from the time of stimulation and it is represented as diamonds, squares and triangles, respectively. These specific times were selected to denote the three phases of the triphasic response.

The electroresponsive structure of the DON

In order to understand how the DON integrates information from the afferent nerve with input from the PF and uses it to eliminate the shark's own electric field we need to analyze the spatial organization of the local field potentials. As described above, the responses to stimulation of the Aff or the PF were characterized at a depth of 500 μm below the surface. Considering the spatial organization of both inputs to the DON, the recorded field potentials are likely to depend on the depth of the recording and the location along the medio-lateral and rostro-caudal axes. Fig. 7 shows an example of local field potentials evoked by stimulating the Aff (Fig. 7A) and the PF (Fig. 7B), and recorded at different depths, starting at the surface of the DON (upper traces) and going down to a depth of 1 mm in increments of 100 μm. The changes in field potentials as a function of recording depth are summarized in Fig. 7C (Aff stimulation) and Fig. 7D (PF stimulation). In each response, we measured three different time points, selected according to the characteristics of the field potential recorded at a depth of 500 μm. Hence, the potentials evoked by Aff stimulation were measured at delays of 3 ms (diamonds), 4 ms (squares) and 6 ms (triangles), corresponding to the first positive peak, the maximal negative peak and the second positive peak, respectively. The potentials evoked by PF stimulation, were measured at 8 ms (diamonds), 12 ms (squares) and 16 ms (triangles), corresponding to the first negative peak, the second positive peak, and the second negative peak, respectively.

Different response characteristics were observed as a function of recording depth. First, at the surface of the DON the response to Aff was characterized by a positive wave that was followed by a small negativity, whereas the response to PF at the same depth lacked the positive peak and was characterized by prolonged negativity. Second, although the fast negativity in both responses (squares in Fig. 7C and diamonds in Fig. 7D) reached maximal amplitude at a depth of about 500 μm, this peak in the PF response decreased rapidly and was diminished by 800 μm (Fig. 7D), whereas this peak in the Aff response was clearly observed at depths below 1000 μm (Fig. 7C). Third, at a depth of 1 mm below the surface, the prolonged negative component in the response to PF stimulation reversed polarity, whereas the response to Aff stimulation decreased substantially without reversing polarity.

The electroresponsive structure of the DON was further analyzed by measuring the responses to Aff stimulation along the rostro-caudal and medio-lateral axes. As shown in Fig. 8, the shape of the field depends on the site of recording as well as the depth of the electrode within the tissue. Specifically, it is apparent that: (1) the nerve terminal potentials were larger at medial locations (arrows in Fig. 8B), suggesting that the Aff input arrives *via* the medial side of the DON; (2) there are very small variations in the response delay recorded along the rostro-caudal axis of the DON (Fig. 8A,B), and these delay variations, which are much smaller than those observed along the medio-lateral axis, suggest that peripheral information arrives simultaneously to all areas along the rostro-caudal plan of the DON; (3) the responses in the lateral DON exhibited a longer

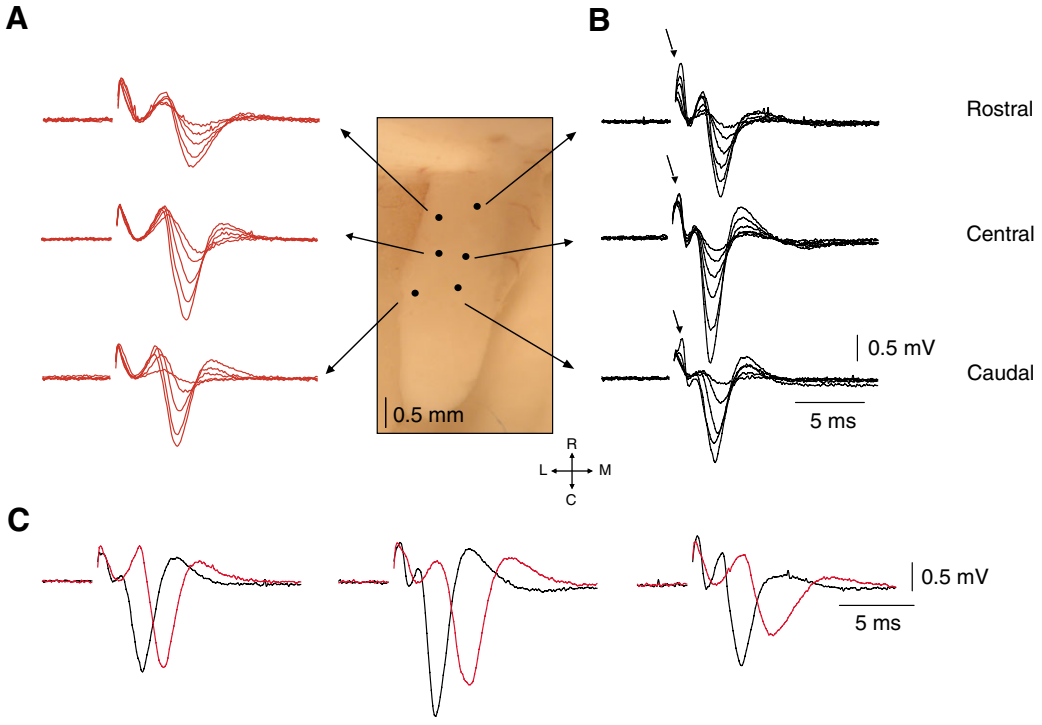

Fig. 8. The response to afferent nerve (Aff) nerve stimulation propagates along the medio-lateral axis. (A,B) The responses to Aff stimulation recorded at three different locations and at 5–6 different depths along the rostro-caudal axis of the lateral (A, red traces) and the medial (B, black traces) sides of the DON. Each record is an average response to eight consecutive stimuli delivered at a rate of 0.1 Hz. The location of each record is marked on a top view of the DON as seen through a dissecting microscope. Arrows in B demark the nerve terminal potential. (C) Superposition of the responses recoded at the medial (black) and lateral (red) locations. Right to left, panels correspond to the three different locations along the rostro-caudal axis. Note the significant delay between the medial and lateral responses. L, lateral; M, medial; R, rostral; C, caudal.

delay and had a wider negative peak compared to those recorded in the medial DON (Fig. 8C). The calculated propagation velocity of the response along the mediolateral axis was 0.26 m s^{-1}, which is rather slow compared to the conduction velocity in the Aff fibers (10.3 m s^{-1}; see above). This suggests that the delay of the response was due to post-synaptic propagation of the signal. Finally (4), the fast negative response was observed in all recorded locations, suggesting that the sites of action potential initiation (likely the soma of the AEN or the ventral dendritic tree) are within the middle portion of the DON at a depth of about 500 μm. It is tempting to speculate that this medio-lateral propagation of the post-synaptic response represents 'back propagation' of action potential along the dorsal dendrite of the AENs.

Short-term interactions between the PF and the Aff inputs

Interactions between the PF and the Aff inputs have been hypothesized to underlie the ability of the DON to extract relevant information from the sensory input (Nelson and Paulin, 1995; Montgomery and Bodznick, 1994). According to these 'adaptive filter' models, feed-forward inhibition in both the PF and the Aff circuits plays a major role in signal adaptation. Therefore, to further understand how the DON processes information we characterized the short-term interactions between these inputs. We measured the responses at the middle portion of the DON where the AEN cell bodies are located (Fig. 3). We implemented paired pulse protocols in which either the Aff nerve or the PF were stimulated. The responses were measured at several time intervals between the two stimuli.

Paired pulse stimulation of the Aff

Paired pulse protocol applied to the Aff nerve revealed significant depression. It reached maximum at about 20 ms and lasted almost 100 ms (Fig. 9A). The amplitude of the response to the second stimulus delivered at 20 ms after the first stimulus, reached 30% of the initial amplitude. The average time course of the depression clearly shows that at 20 ms it is larger than at 10 ms (Fig. 6C; *N*=9). The maximum depression averaged over nine preparations was 68.6±15.2%. The amplitude of the second response gradually increased with the interval between the two stimuli while maintaining the shape of the initial response, suggesting that the depression Affects all stimulated components equally. Moreover, a second negative peak (Fig. 9A, arrows) appeared in the response to the second stimulus. This second peak indicates the presence of a facilitatory process occurring in addition to inhibition of the AENs.

The delayed peak of the depression indicates that it is

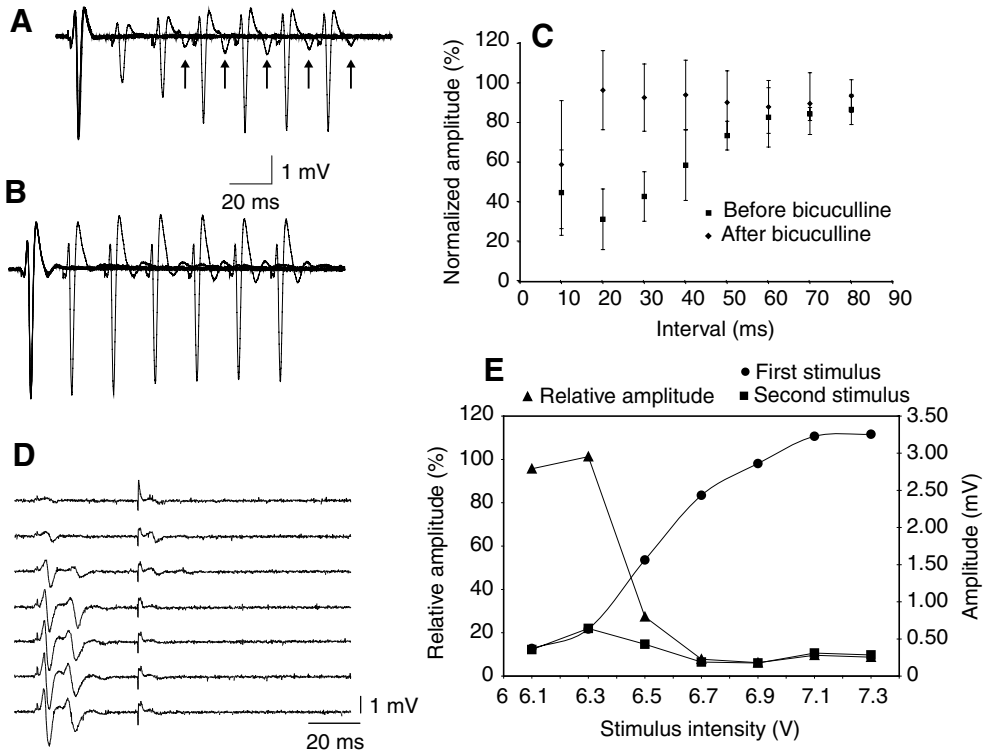

Fig. 9. Bicuculline-sensitive inhibition induced by afferent nerve (Aff) nerve stimulation. (A,B) Superimposed traces of the responses to paired pulse stimulation of the Aff nerve. The paired stimuli were delivered at 20, 40, 60, 80, 100 and 120 ms intervals. Each record is an average response to eight consecutive stimuli delivered at a rate of 0.1 Hz. Arrows denote the second negative peak that increased as a function of the paired pulse interval. (A) Before and (B) after the addition of bicuculline (100 μmol l^{-1}). (C) The amplitude of the responses to the second stimulus, normalized by the amplitude of the first response, as a function of the inter-stimuli interval. Diamonds indicate responses before, and squares, responses after addition of bicuculline. *N*=9 (control), *N*=7 (+bicuculline). (D,E) The inhibition induced by Aff stimulation increases as a function of stimulus intensity. (D) The responses to a pair of stimuli delivered to the Aff at an interval of 40 ms. Each trace shows the response to different stimulus intensity, increasing from top to bottom. (E) The amplitude (right axis) of the response to the first (circles) and second (squares) stimulus as a function of stimulus intensity. Triangles indicate the relative amplitude of the second response (left axis) as a function of stimulus intensity.

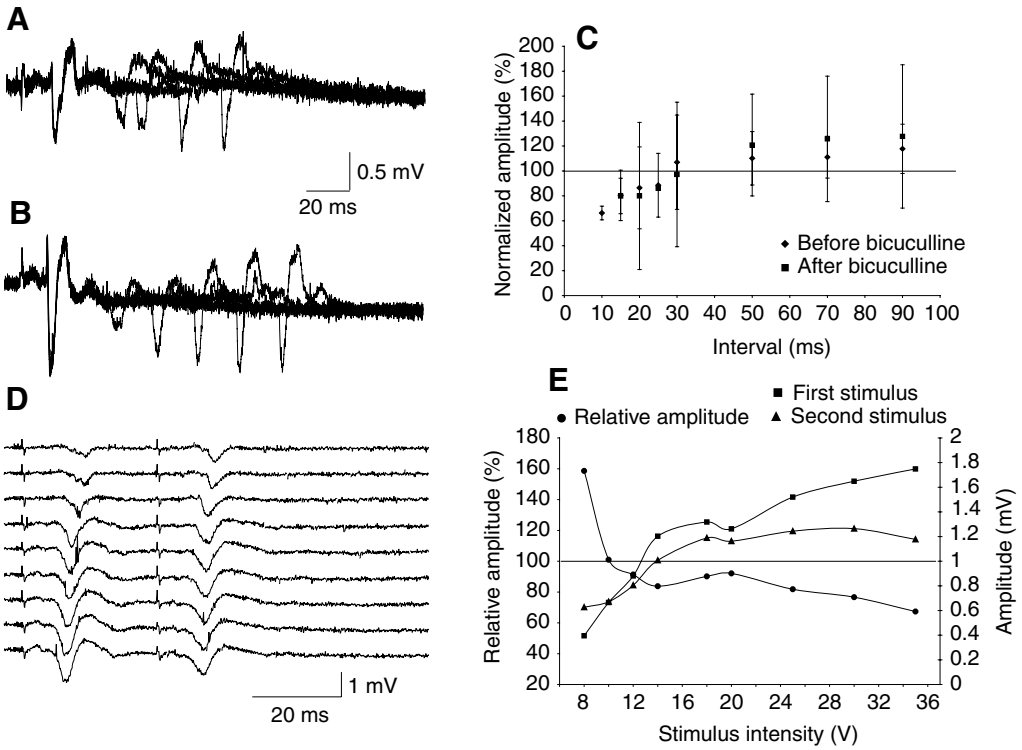

Fig. 10. Bicuculline-insensitive inhibition induced by parallel fibers (PF) stimulation. (A,B) Superimposed traces of the responses to paired pulse stimulation of the PF. The controlled paired stimuli in A were delivered at 30, 40, 60 and 80 ms intervals. The paired stimuli in the presence of bicuculline (100 μmol l^{-1}) (B) were delivered at 30, 50, 70, 90 and 110 ms intervals. Each record is an average response to eight consecutive stimuli delivered at a rate of 0.1 Hz. (C) The amplitude of the responses to the second stimulus, normalized by the amplitude of the first response, as a function of the inter-stimuli interval. Diamonds indicate responses before, and squares, responses after addition of bicuculline. *N*=9 (control), *N*=3 (+bicuculline). (D) The responses to a pair of stimuli delivered to the PF at an interval of 30 ms. Each trace shows the response to different stimulus intensity, increasing from top to bottom. (E) The amplitude (right axis) of the response to the first (circles) and second (squares) stimulus as a function of stimulus intensity. Triangles indicate the relative amplitude of the second response (left axis) as a function of stimulus intensity.

mediated *via* chemical synapses. We therefore examined the effect of bicuculline, a commonly used GABAergic blocker, on the inhibition measured by paired pulse protocol. Bicuculline completely abolished the inhibition (Fig. 9B,C). Nonetheless, at an interval of 10 ms, the amplitude of the response remained smaller than the initial response despite the presence of bicuculline. This reduction in amplitude is probably due to refractory period. Furthermore, the amplitude of the response to the first stimulus increased (compare Fig. 9A with Fig. 9B), suggesting that the feed-forward inhibition is fast enough to decrease significantly the initial excitatory response or that some of the GABAergic receptors on AENs are tonically active. On average, after blocking the $GABA_A$ receptors the amplitude of the response to Aff stimulation increased by 22.2±12.2% (*N*=5; *P*<0.002). The fast onset of the inhibitory response suggests that the inhibitory neurons have a low threshold and a short time constant. To further elucidate the source of inhibition, we examined the dependence of inhibition on Aff stimulus intensity. In the example shown in Fig. 9D, the inhibition evoked by Aff stimulation was measured at 40 ms intervals. The amplitudes of the first response (circles), the second response (rectangles) and their ratio (triangles) are shown in Fig. 9E. The inhibitory effect started at very low stimulus intensities. The response to the first stimulus increased monotonically with stimulus intensity while the response to the second stimulus was rather small, even at high stimulus intensities, and was intensity independent. Thus, we suggest that the inhibition evoked by Aff nerve stimulation is highly efficient and is widely distributed throughout the DON.

Paired pulse stimulation of the PF

A similar paired pulse protocol was applied to the PF. As shown in Fig. 10, stimulating the PF evoked a short period of suppression that persisted in the presence of bicuculline. The suppression evoked by PF stimulation was significantly smaller than the inhibition induced by Aff stimulation. The response to the second PF stimulation decreased by 33.8±5.4% on average (*N*=3). The suppression was most effective at a short interval of 10 ms and decayed exponentially with a time constant of 10–20 ms (Fig. 10C). Similar to Aff stimulation, at long time intervals the response to the second pulse was larger than the initial response, implying the emergence of facilitation (Fig. 10C). Bicuculline increased the response to the first stimulus but did not effect the suppression evoked by the paired pulse protocol (*N*=3; Fig. 10B,C). As with Aff stimulation, the suppression depended on stimulus intensity (Fig. 10D,E). At low intensities the paired pulse protocol revealed a significant facilitation rather than suppression (the relative amplitude of the

second response reached 160%, N=3; P<0.01). At medium stimulus intensities of about 50% above threshold, the suppression decreased the amplitude of the second response by 10–20%. At stronger stimulus intensities, the inhibition increased further and reached a maximum of about 30%. Considering the short duration of this effect, its characteristic dependence on stimulus intensity and its insensitivity to bicuculline, it is likely that the suppression activated by paired pulse stimulation of PF is due to a refractory period and not activation of an inhibitory pathway.

Discussion

In this work we introduce a novel and unique experimental system that combines the advantages of *in vitro* preparations with the integrity of the *in vivo* approach. Similar to slice preparations, the isolated DON offers stable recording conditions, accessibility for drug manipulation and the feasibility to implement modern recording techniques. Yet, unlike slice preparations, the isolated DON retains an intact circuitry including the Aff nerve. Retaining an intact Aff is critical to ensure controlled activation of the electroreceptor pathway. Hence, in this experimental setup it is possible to study the responses in the DON to activation of the PF and the Aff and the mechanisms underlying their long-term interactions.

The electroresponsive architecture of the DON

We have demonstrated that the PF input is located at the dorsal surface of the DON whereas the Aff input is probably located deeper in the ventral side of the nucleus. We have also shown that the response to Aff nerve stimulation propagates along the medio-lateral axis of the DON. These observations are summarized in the quasi-schematic representation in Fig. 11, superimposed on a micrograph of the DON cross-section. The cell bodies of its principal neurons, the AEN (Fig. 11, thick red line), are located in the middle portion of the DON. Based on our histology (Fig. 3) and electrophysiology data (Fig. 8), the dorsal dendrites of the AEN extend up into the molecular layer located at the top of the cross section (marked by green dots). The information arriving *via* the Aff reaches the ventral dendrites of the AEN at the bottom layer of the DON (marked in yellow). Assuming that the trajectory of recording electrode was as shown in Fig. 11 (broken line), the synaptic response within the molecular layer is expected to be negative (sink) during PF stimulation and positive (source) during Aff nerve stimulation, as shown in Fig. 7. It is also expected that the generation of action potentials at the AEN's soma will cause a negative wave in the middle portion of the DON. Indeed, both PF and Aff stimulation induced a negative response in this part of the DON. Nonetheless, due to location of the electrode that stimulates only a beam of PF, the response to PF was markedly attenuated once the recording electrode crossed the border between the molecular layer and the cell body layer. At this point the deeper AEN dendrites are not activated by the PF-stimulating electrode. In contrast, when the Aff is stimulated, it activates most of the AEN; therefore, the response to Aff nerve stimulation could be detected deep inside the DON area, which was not activated by the surface electrodes that stimulated only a narrow beam of PF. The possibility that the action potential back-propagates along the dorsal dendrite could also contribute

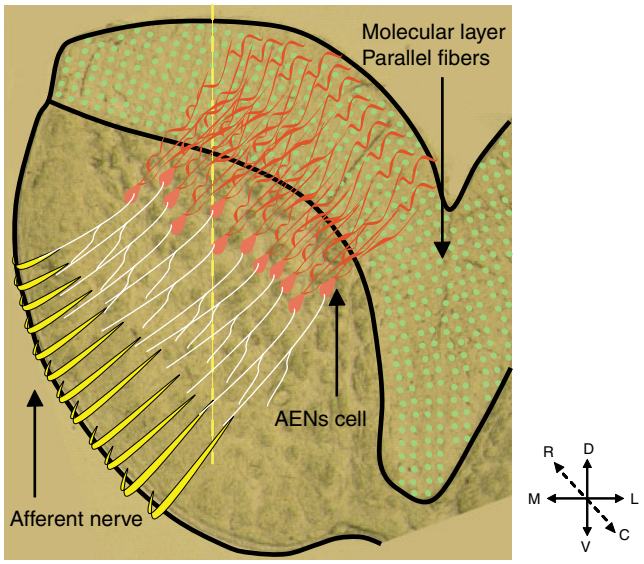

Fig. 11. Quasi-schematic representation of the electroresponsive structure of the DON. Schematic representation of the postulated neuronal circuitry superimposed on a cross-section of the DON. The molecular layer at the top of the cross section (green dots) is the location of all the apical dendrites of the principal neurons. The elongated cell bodies (in red) are located at the middle of the DON and the incoming afferent nerve innervates the basal dendrites in the deep layer (in yellow). The broken yellow line delineates a hypothetic path of the recording. AEN, ascending efferent neurons; D, dorsal; V, ventral; L, lateral; M, medial; R, rostral; C, caudal.

to the fact that the Aff response can be detected throughout the dorso-ventral axis of the DON. It is expected that the current flow of the back-propagating action potentials, activated by the Aff input, will be different from the forward-propagating action potentials activated by the PF. Non-symmetric arrangement of the inputs and several spike initiation sites will cause the relationship between the different components of the field potential evoked by Aff to be different from those evoked by PF.

The PF input to the DON

There are four properties of the PF input that should be discussed: the conduction velocity, the dependence on stimulus intensity, the kinetics of the response, and the activation of feed-forward inhibition. Since the DON is regarded as a component of the elasmobranch cerebellum (Bell, 2002; Paulin, 1993), the properties of the PF are expected to resemble those of cerebellar PF. Indeed, the measured conduction velocity of 0.13 m s^{-1} is similar to 0.2 m s^{-1} measured in dogfish *Scyliorhinus canicula* (Paul, 1969), 0.2 m s^{-1} in frogs (Llinas et al., 1969) and 0.3 m s^{-1} in cats (Eccles et al., 1966). As in the cerebellum, the number of PF is quite large while each fiber seems to form low efficacy synapses. This can explain the high stimulus intensity required to evoke a response when the PF were stimulated (see Figs 4 and 5); many fibers should be activated in order to evoke a detectable postsynaptic response. It also explains the almost linear relationship between stimulus intensity and response amplitude. Unlike cerebellar Purkinje cells, the AEN's response to PF stimulation is characterized by multiple peaks, suggesting

that the dorsal dendrites may produce complex regenerative activity. Indeed the intracellular recordings (Fig. 5F) show that the burst of action potentials that was evoked at high stimulus intensity was elicited by a prolonged plateau-like depolarization that lasted much longer than the underlying synaptic potential. The significant decrease in the delay of the response that occurred when stimulus intensity was increased (Fig. 4D) suggests a slow kinetics of the synaptic input. A slow rise time of synaptic potential will generate a significant decrease in the delay as the time to reach the threshold decreases with the increase in amplitude. This interpretation of the LFP response was confirmed by intracellular recordings showing that the rise time of the PF synaptic potential is twice as long as the Aff synaptic potential (Fig. 5E). Finally, paired pulse protocol delivered to the PF system revealed two types of interactions: an inhibitory interaction at high stimulus intensities and facilitatory interaction at low intensities. The facilitation may represent an increase in synaptic transmission and or the summation of prolonged synaptic potential. The latter possibility is supported by the exceptionally prolonged field potential (see Fig. 2B), which can last for over 100 ms, and the plateau-like depolarization (Fig. 5E). The inhibitory interactions occurred at high stimulus intensities, peaked immediately after the stimulus and decayed exponentially with a time constant of 10–20 ms. The inhibitory effect of the PF on themselves and on the response to Aff nerve stimulation had a similar time course and was insensitive to bicuculline. These observations suggest that the inhibitory effect evoked by PF stimulation represents inactivation of the regenerative responses in the AEN (Poulter et al., 1993), rather than activation of inhibitory synapses. However, the possible involvement of glycine receptors should be examined.

The Aff input to the DON

The Aff nerve that transmits the peripheral information to the DON has a low threshold and a high conduction velocity. A conduction velocity of 10.3±4.4 m s^{-1} measured in our isolated preparation is within the range of conduction velocities measured in peripheral nerves of other species such as frogs (10 m s^{-1}) (Poulter et al., 1993) and mammals (30–80 m s^{-1}) (Nicholls et al., 2001). This high conduction velocity is also in accordance with the high rate of activity observed *in vivo* in this preparation (Tricas and New, 1998). The rather low threshold and rapid saturation of the response (Fig. 4E and Fig. 5C) can be explained by assuming that the number of afferent terminals that innervate a given area of AEN neurons is rather small compared to the number of PF that innervate the same area. A low number of Aff nerve terminals will cause the field potential to saturate at low stimulus intensities, as observed (see Fig. 4). The low threshold causes the AENs to be easily activated by Aff input and suggests that a small number of fibers is required to activate the AENs. This possibility was further supported by the intracellular recordings, which show that action potentials in AEN are triggered by a rather low amplitude synaptic potential (see Figs 2 and 5) that attained a limited number of possible amplitudes. The latter strongly suggests that each AEN is innervated by a small number of Aff terminals. This conclusion argues against one of the mechanisms postulated in the adaptive filter model of the DON. According to this mechanism, the output of the DON occurs only when the Aff input integrates with the PF input. A very low threshold of the Aff input will leave no range for integration with PF input. On the other hand, the low threshold of the Aff input supports the inhibition role in this model. If the threshold is low and there are few inputs, an inhibitory input located at a strategic site can act as an efficient gatekeeper, enabling only unpredicted information to pass through the gate.

The sharp negative wave in the field potential, which characterizes the response to Aff stimulation, suggests that synaptic input is relatively fast and synchronized. This possibility is further supported by the insensitivity of the delay of the response to stimulus intensity, and it is clearly demonstrated in the intracellular recordings. Hence, we can conclude that the Aff input has a low threshold for activation of the AEN neurons and relatively fast kinetics. It is located at the ventral dendrites of the AENs and each neuron is innervated by a small number of afferent axons.

Threshold differences are one of the most remarkable observations. In order to activate the neuron by PF input, the membrane had to be depolarized by 12 mV, as measured at the recording site. However, only 3 mV of membrane depolarization was needed to activate the neurons when Aff was stimulated. Such a fourfold difference in threshold is a puzzling result. The most straightforward possibility is that the spike initiation site is located closer to the location of the Aff input. This simple explanation is supported by the fact that presumed axons seem to emerge from a ventrally oriented dendrite (Fig. 3) and agrees with the rather superficial recording site. On average, the recording electrode was located 200 μm below the surface. We assume that at this depth the electrode is still within the molecular layer. Therefore we have to conclude that most of the recordings were performed from dorsal dendrites. This possibility is in agreement with the recording of relative large PF synaptic potentials. From the site of recording, this synaptic potential will passively propagate toward the cell body and down the ventral dendrite to the presumed site of spike initiation. Such a passive propagation over a rather long distance will lead to voltage attenuation and thus, at the site of spike initiation, the voltage threshold is similar for all inputs. This explanation can also account for the similarity between the threshold for direct current injection and the PF threshold. From the site of recording these two signals have to propagate along the same path to reach the site of spike initiation and therefore will have to be of similar amplitude. Small variations between these two signals can be reconciled by assuming that the PF input is distributed all over the dorsal dendrites whereas the current injection is limited to one point only. However, the rise time of the Aff synaptic potential is shorter than that of the PF synapse. The cable theory demonstrated that the rise time of synaptic events is the most sensitive parameter that is affected by the electrotonic distance. If two inputs that have the same kinetics are distributed in space, the proximal input will have a faster rise time. Accordingly the faster rise time of the Aff synaptic potential implies that the Aff input is located closer to the recording site.

This conclusion is in sharp contrast to the observations summarized above. For this reason we are force to conclude either the Aff input has faster kinetics or that there are two

different spiking mechanisms, one with high threshold located close to the PF input and the other with low threshold located closer to the Aff input. It is interesting to note that in a very recent publication, Bell and his colleagues (Zhang et al., 2007) show that the afferent input in an analogous electrosensory structure in teleosts fishes has an electrotonic component. Such a mechanism can account for a rather fast rise time of the Aff synaptic potential.

The Aff nerve activates inhibitory pathways that exert significant inhibition on the Aff input. This feed-forward inhibition has several unique properties. First, it peaks after 20 ms from the stimulus onset. Such delay onsets are usually associated with metabotropic type of receptors; however, the complete blockade of this inhibition by bicuculline argues against this possibility. An alternative posibility to account for the prolongued delay is that the inhibition is activated *via* feedback mechanisms from the AEN to the midbrain through the DGR back to the DON. Second, although this inhibition is highly effective and can eliminate up to 90% of the Aff response, it does not affect the PF response. This is a puzzling result, which argues against the possibility of inhibition through the DGR, and can be explained by activation of presynaptic inhibition that limits the effect to the Aff terminals, and/or by activation of feed-forward inhibition that is located at distal compartments of the ventral dendrites (i.e. close to the site of Aff input and remote from the site of PF input). The latter possibility implies that the spike initiation zone of the PF input differs from that of the Aff input. The absence of inhibitory synaptic potentials in the intracellular recordings supports both possibilities.

Further study is required to understand the synaptic mechanisms of the inhibitory and excitatory inputs in this unique preparation. However, it is clear that our data do not support the cancellation mechanism suggested in the adaptive filter model of the DON (Montgomery and Bodznick, 1994; Nelson and Paulin, 1995). Alternative models, according to which parallel fibers adjust the response properties of the Purkinje-like AENs, have been suggested (Paulin, 2005; Paulin and Nelson, 1993; Paulin et al., 1998). These alternative models are consistent with experimental evidence (Bastian, 1986; Bower, 2002; Santamaria and Bower, 2005) about neuronal interactions in cerebellum and cerebellar-like sensory filtering structures.

Funding provided by the Minerva Stiftung (BMBF German Federal Ministry for Education and Research) and the Hebrew University.

References

Bastian, J. (1986). Gain control in the electrosensory system mediated by descending inputs to the electrosensory lateral line lobe. *J. Neurosci.* **6**, 553-562.

Bell, C. C. (2002). Evolution of cerebellum-like structures. *Brain Behav. Evol.* **59**, 312-326.

Bodznick, D., Montgomery, J. C. and Tricas, T. C. (2003). *Sensory Processing in Aquatic Environments* (ed. S. P. Collin and N. J. Marshall). New York: Springer-Verlag.

Bower, J. M. (2002). The organization of cerebellar cortical circuitry revisited: implications for function. *Ann. N. Y. Acad. Sci.* **978**, 135-155.

Devor, A. (2000). Is the cerebellum like cerebellar-like structures? *Brain Res. Brain Res. Rev.* **34**, 149-156.

Eccles, J. C., Llinas, R. and Sasaki, K. (1966). The action of antidromic impulses on the cerebellar Purkinje cells. *J. Physiol.* **182**, 316-345.

Hentschel, H., Nearing, J., Harris, H. W., Betka, M., Baum, M., Hebert, S. C. and Elger, M. (2003). Localization of Mg^{2+}-sensing shark kidney calcium receptor SKCaR in kidney of spiny dogfish, *Squalus acanthias*. *Am. J. Physiol.* **285**, F430-F439.

Llinas, R., Bloedel, J. R. and Hillman, D. E. (1969). Functional characterization of neuronal circuitry of frog cerebellar cortex. *J. Neurophysiol.* **32**, 847-870.

Montgomery, J. C. (1984). Noise cancellation in the electrosensory system of the thornback ray; common mode rejection of input produced by the animal's own ventilatory movement. *J. Comp. Physiol. A* **155**, 103-111.

Montgomery, J. C. and Bodznick, D. (1994). An adaptive filter that cancels self-induced noise in the electrosensory and lateral line mechanosensory systems of fish. *Neurosci. Lett.* **174**, 145-148.

Montgomery, J. C. and Bodznick, D. (1999). Signals and noise in the elasmobranch electrosensory system. *J. Exp. Biol.* **202**, 1349-1355.

Nelson, M. E. and Paulin, M. G. (1995). Neural simulations of adaptive reafference suppression in the elasmobranch electrosensory system. *J. Comp. Physiol. A* **177**, 723-736.

Nicholls, J. G., Martin, A. R., Wallace, B. G. and Fuchs, P. A. (2001). *From Neuron to Brain*. Sunderland, MA: Sinauer Associates.

Paul, D. H. (1969). Electrophysiological studies on parallel fibers of the corpus cerebelli of the dogfish *Scyliorhinus canicula*. In *Neurobiology of Cerebellar Evolution and Development* (ed R. R. Llinas), pp. 245-249. Chicago: American Medical Association.

Paul, D. H. and Roberts, B. L. (1977). Studies on a primitive cerebellar cortex. I. The anatomy of the lateral-line lobes of the dogfish, *Scyliorhinus canicula*. *Proc. R. Soc. Lond. B Biol. Sci.* **195**, 453-466.

Paul, D. H., Roberts, B. L. and Ryan, K. P. (1977). Comparisons between the lateral-line lobes of the dogfish and the cerebellum: an ultrastructural study. *J. Hirnforsch.* **18**, 335-343.

Paulin, M. G. (1993). The role of the cerebellum in motor control and perception. *Brain Behav. Evol.* **41**, 39-50.

Paulin, M. G. (2005). Evolution of the cerebellum as a neuronal machine for Bayesian state estimation. *J. Neural Eng.* **2**, S219-S234.

Paulin, M. G. and Nelson, M. E. (1993). Combining engineering models with biophysical models to analyse a biological neural network: the electrosensory system of sharks, skates and rays. In *Proceedings of the First New Zealand International Two-Stream Conference on Artificial Neural Networks and Expert Systems.* doi: 10.1109/ANNES.1993.323094.

Paulin, M. G., Senn, W., Yarom, Y., Meiri, H. and Cohen, D. (1998). A model of how rapid changes in local input resistance of shark electrosensory neurons could enable the detection of small signals. In *Computational Neuroscience 1998* (ed. J. Bower), pp. 239-244. New York: Plenum.

Poulter, M. O., Hashiguchi, T. and Padjen, A. L. (1993). An examination of frog myelinated axons using intracellular microelectrode recording: the role of voltage-dependent and leak conductances on the steady-state electrical properties. *J. Neurophysiol.* **70**, 2301-2312.

Santamaria, F. and Bower, J. M. (2005). Background synaptic activity modulates the response of a modeled purkinje cell to paired afferent input. *J. Neurophysiol.* **93**, 237-250.

Tricas, T. C. and New, J. G. (1998). Sensitivity and response dynamics of elasmobranch electrosensory primary afferent neurons to near threshold fields. *J. Comp. Physiol. A* **182**, 89-101.

Zhang, J., Han, V. Z., Meek, J. and Bell, C. C. (2007). Granular cells of the Mormoryd sensory lobe and postsynaptic control over presynaptic spike occurrence and amplitude through an electrical synapse. *J. Neurophysiol.* **97**, 2191-2203.